A Vision Problem in Wire Bonding

Norliza Mohd. Noor
Program Pengajian Diploma,
Universiti Teknologi Malaysia, Kampus Semarak, Jalan Semarak
54100 Kuala Lumpur
e-mail: norliza@utmnet.utm.my

Ass. Prof. Dr. Omar Mohd. Rijal
Institute of Mathematical Science
University Malaya
Lembah Pantai
59000 Kuala Lumpur

Omar Mohd. Badar
Texas Instrument (M)
Hulu Kelang Free Trade Zone
68000 Selangor D.E.
e-mail: omar@ti.com

P'ng Yik Thon
Institute of Mathematical Science
University Malaya
Lembah Pantai
59000 Kuala Lumpur
e-mail: pngyt@tm.net.my

Abstract: A requirement for good wire bonding is the existence of intermetallics between the gold ball and bond pad. A digital image of the surface of the gold ball that was attached to the bond pad was obtained and analysed with MATLAB.

The 'counting method' (CM) is proposed for determining the percentage of intermetallics formation. Four experiments were performed to investigate the reliability of CM, the effect of light-offset, and the performance of a Quality Assistant (QA) in his ability to visually estimate (the visual method) the intermetallics coverage.

The main results indicate that the visual method is inconsistent and less accurate than the counting method. The QA performs well for high intermetallics coverage, whilst for an approximately 50% intermetallics coverage the QA tends to over-estimate.

Critical remarks related to modeling the digital image are presented.

Keywords: Gold-Aluminum Wire bonding, intermetallics formation, visual estimation, image histograms, statistical modeling.

I. Introduction

The present study is motivated by the results in [1]. In particular it is shown in [1] that visual interpretations (inference) is dependent on the experimenter (observer), output media and intensity of images. However the simulated images in [1], may be regarded as an example of a 'complicated' case study, constraining attempts at investigating the problem of image perception. In this paper, the image for the wire bonding problem is considered a 'simple' case study, thus allowing the opportunity for more objective approaches.

Intermetallics of gold (Au) and aluminum (Al) are initiated during the bonding process. The formation of Au-Al intermetallics is the process that causes the bond between gold wire and 'substrate' to stick or adhere.

In order to view the intermetallics coverage of the ball, the ball bond needs to be removed from the bond pad without destroying the intermetallics. Etching the bond pad of a well-bonded leadframe sample in a 25% potassium hydroxide (KOH) solution achieves this. The etching process requires approximately 20 to 30 minutes.

II. The Visual Method

Table 1 gives the range of color when gold and aluminum combine to form the intermetallics compounds.

For the visual method, a photograph of the image is made. Then a square matrix is overlaid on the photo and the squares within the edge of the bonded ball that contain intermetallics are counted. The ratio of the intermetallics area to that of the total area is defined as the percentage intermetallics (%IM).

Table 1: Intermetallics compound formed in Au-Al bond [2].

Compound	Color
Au (gold)	
Au_4Al	White
Au_5Al_2	Off White
Au_2Al	Dark Brown
AuAl	Light Tan
$AuAl_2$	Purple
Al	

III. The Counting Method (CM)

The digital image of the bonded ball surface is used in the CM-method. Employing the software MATLAB, a circle that contains the whole gold ball area is fitted into the entire image. This procedure finds a center, determines a radius such that the background area is minimized. Then the program will start counting the pixels beginning from the upper-left corner to the bottom-right corner of the image.

A typical example of the 'circled' image is given in Fig. 1(a), and its corresponding image histogram in Fig. 1(c). The area under the middle hump of the image histogram is of main concern.

IV. Some experiments using red-band image

Several experiments were carried out with details outlined in [3]. Amongst the results are:

(i) the threshold points (cut-off points) to determine the 'middle hump' may be varied within small intervals such that the %IM does not very significantly. In other words, the image histogram is a fairly robust tool for determining %IM,

(ii) different percentage of light offsets (0%, 9%, 21%, 31% and 40%) used to capture the image does not significantly vary the estimates for %IM. However the 50% light-offset is an exception,

(iii) when the intermetallics coverage is high, both methods perform similarly. However when the coverage is low (approximately 50%) the visual method may be inaccurate or inconsistent.

V. Automatic Determination Of Threshold Points

The tedious process of determining threshold points by trial and error warrants a more systematic and automatic procedure. One possible approach is to fit mixture-distributions for the image histogram, and hence the threshold points may be determined using ideas of statistical discrimination (see [4]).

The QA with his visual method does his estimation of the %IM with the RGB image. Unfortunately managing (manipulating) the RGB images is time-consuming and therefore we look at the histograms for the red, green and blue band respectively for an efficient alternative. Confining the discussion to the circled images, we see that comparing Fig. 1(c), Fig. 2(c), Fig. 3(c) and Fig. 4(c), the histogram of the red band image is most similar to that of the RGB image.

The red band histogram may be regarded as a reasonable model of the image in the following sense; there are three (main) representative regions:

(i) the left most hump represents the background between the circle-boundary and the edge of the ball bond,

(ii) the middle hump represents the intermetallics phases, and

(iii) the steep curve on the right most likely represents the final Au_4Al stage.

Henceforth we propose fitting a three component normal mixture to a red band histogram and the histogram chosen is given in Fig. 7. The model fitted is;

$$f(x) = p_1 g_1(x) + p_2 g_2(x) + p_3 g_3(x)$$

where $g_k \sim N(\mu_k, \sigma_k^2)$ $\quad k = 1,2,3$

and $\sum_{j=1}^{3} p_j = 1$.

Following [5] we can show that the maximum likelihood parameter estimates are given as follows:

Let $x_1, x_2, \ldots, x_n$ be grey-level values. By Bayes theorem,

$$\Pr(k \mid x_j) = \frac{p_k g_k(x_j \mid \mu_k, \sigma_k^2)}{f(x_j)}$$

$$\hat{p}_k = \frac{1}{n}\sum_{j=1}^{n} \Pr(k \mid x_j) \qquad \Lambda\ (1)$$

$$= \frac{1}{n}\sum_{j=1}^{n} \frac{\hat{p}_k g_k(x_j \mid \hat{\mu}_k, \hat{\sigma}_k^2)}{f(x_j)}$$

$$\hat{\mu}_k = \frac{1}{n\hat{p}_k}\sum_{j=1}^{n} \frac{x_j \hat{p}_k g_k(x_j, \hat{\mu}_k, \hat{\sigma}_k^2)}{f(x_j)} \qquad \Lambda\ (2)$$

and

$$\hat{\sigma}_k^2 = \frac{1}{n\hat{p}_k}\sum_{j=1}^{n} \frac{(x_j - \hat{\mu}_k)^2 \hat{p}_k g_k(x_j : \hat{\mu}_k, \hat{\sigma}_k^2)}{f(x_j)} \qquad \Lambda\ (3)$$

Equations (1), (2) and (3) are solved iteratively using the EM algorithm.

The mixture distribution obtained is given in figure 8; clearly shown to be a bad fit. Table 2 gives initial and final parameter estimates. Clearly the middle hump in Fig. 7 is badly estimated. However instead of immediately seeking alternative forms for $g_k(x)$, k = 1,2,3 we have a re-look at the original data.

VI. Reinvestigating the data

We propose two possibilities that may yield a histogram that could represent the data more accurately, namely;

(i) replace the circle image with a polygon image,

(ii) consider histogram in the green band and blue band, and

(iii) consider separately all three bands given that we have low %IM and high %IM.

The polygon image was obtained using a function in MATLAB software where the user captures the region of interest by clicking the cursor around the intermetallics area. This will provide as a mask to the original image where inside the region of interest is represented as '1' and outside as '0'. The mask and the original image is then multiplied together leaving intermetallics area in the original pixel value and the rest (outside the area) all represented by '0' pixel value.

VII. Discussion and further remarks

This study seeks an automatic and efficient procedure of estimating %IM. The approach used involved modeling the histogram with a mixture distribution. The pertinent results obtained are;

(i) the method of preprocessing the image (circle or polygon) effects the shape of the histogram, compare Fig.1(c) and Fig. 1(d). The polygon image give a simpler model,

(ii) for the polygon image, all three color band exhibit different histograms, see Fig. 1(d), Fig. 2(d), Fig. 3(d) and Fig. 4(d), and

(iii) images with low %IM (green band) differ from images with high %IM, see Fig. 5(e) and Fig. 6(e).

In conclusion although the image histogram is a fairly robust tool for determining %IM, unfortunately modeling the histogram with mixture distributions is non-trivial. As a possible aid in choosing the appropriate (representative) histogram (i.e. which color band for a given %IM and a given polygon image) our result suggest two approaches. Firstly, create (or model) a set of representative histograms, for example Fig. 5(e) indicates low %IM and Fig. 6(e) indicates high %IM, and a look up table could then be created. Secondly, the result of [6] suggests considering the thickness of the intermetallics and the result of [7] suggest investigating the circumference of the intermetallics area as covariates. Investigating the relationships between (i) %IM and thickness of intermetallics, and (ii) %IM and circumference forms the next phase of this study.

References

[1] O.M. Rijal and N.M. Noor, "Modeling the R.O.C. curve to investigate image perception", The Proceedings of 1995 IEEE Singapore International Conference On Signal Processing, Circuits And Systems, (IEEE SICSPCS '95), Singapore, 1995, pp.265-267.

[2] R. Howard, "Gold Ball Bonder Benchmark": Technical Report, Interconnection Process Lab, Process Automation Center, Semiconductor Group, Texas Instruments, 1995, pp.33-36, pp. 110-112.

[3] O.M. Rijal, N.M. Noor, O.M. Badar and Y.T. P'ng, "Digital image analysis for measuring intermetallics formation": Technical Report, Assembly Technical Department, Texas Instruments Malaysia, 1999.

[4] T.W. Anderson, An Introduction To Multivariate Statistical Analysis, John Wiley & Sons, 1958, pp. 126-152.

[5] B.S. Everitt and D.J. Hand, Finite Mixture Distributions, Chapman and Hall, 1981.

[6] T. Ramsey, C. Alfaro and H. Dowell, "Metallurgy's Part In Gold Ball Bonding", Semiconductor International, April 1991, pp. 98-102.

[7] G.V. Clatterbaugh, J.A. Weiner and H.K. Charles, "Gold-Aluminum Intermetallics: Ball Bond Shear Testing And Thin Film Reaction Couples", IEEE Trans. on Components, Hybrids and Manufacturing Technology, No. 4, 1984, pp. 349-356.

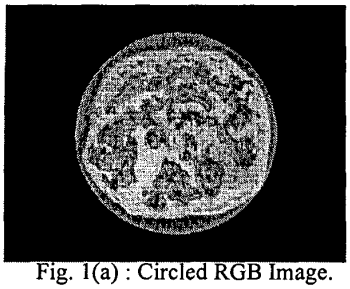

Fig. 1(a) : Circled RGB Image.

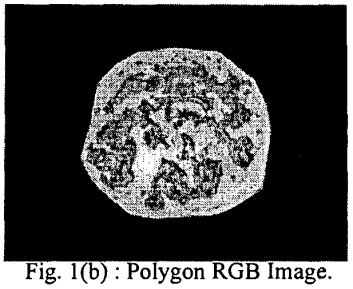

Fig. 1(b) : Polygon RGB Image.

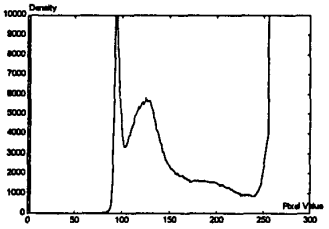

Fig. 1(c) : Density Histogram of Fig. 1(a).

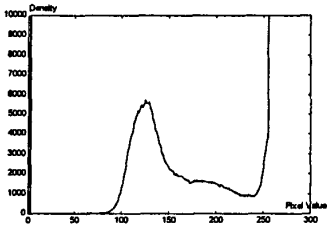

Fig. 1(d) : Density Histogram of Fig. 1(b).

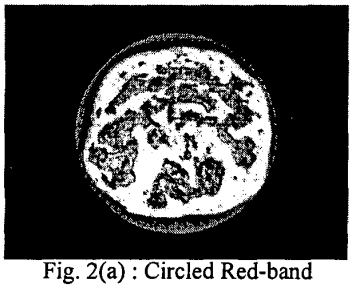

Fig. 2(a) : Circled Red-band Image (Low IM).

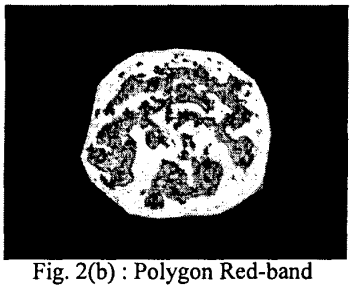

Fig. 2(b) : Polygon Red-band Image (Low IM).

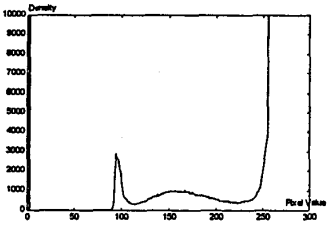

Fig.2(c) : Density Histogram of Fig. 2(a).

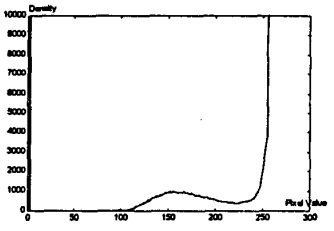

Fig. 2(d) : Density Histogram of Fig. 2(b).

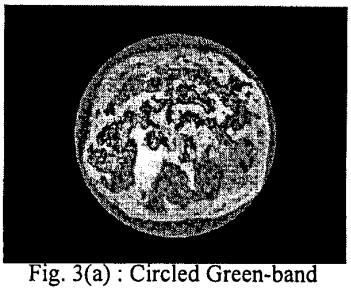

Fig. 3(a) : Circled Green-band Image (Low IM).

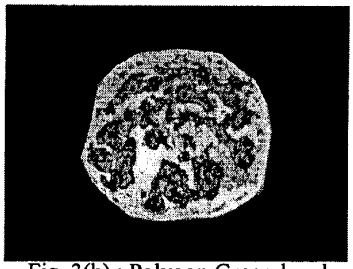

Fig. 3(b) : Polygon Green-band Image (Low IM).

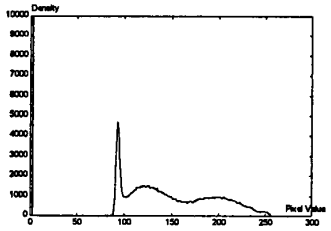

Fig.3(c) : Density Histogram of Fig. 3(a).

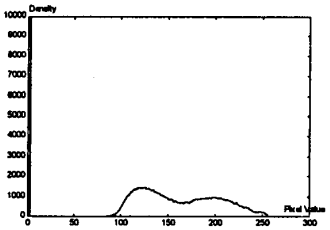

Fig. 3(d) : Density Histogram of Fig. 3(b).

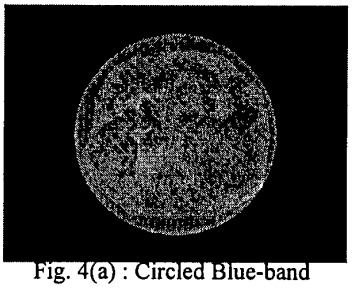

Fig. 4(a) : Circled Blue-band Image (Low IM).

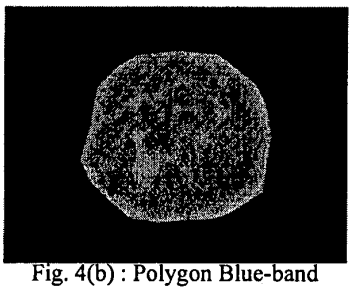

Fig. 4(b) : Polygon Blue-band Image (Low IM).

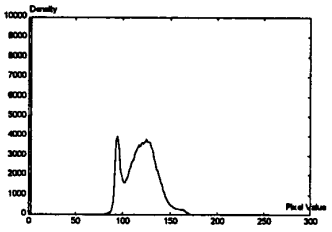

Fig.4(c) : Density Histogram of Fig. 4(a).

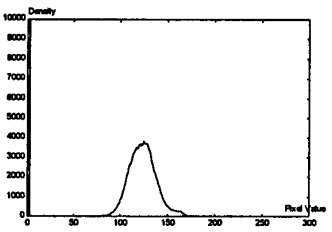

Fig. 4(d) : Density Histogram of Fig. 4(b).

Fig. 5(a) : Polygon Red-band Image (Low IM).

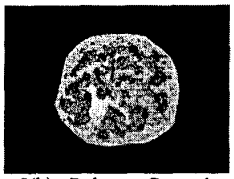

Fig. 5(b) : Polygon Green-band Image (Low IM).

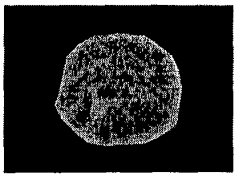

Fig. 5(c) : Polygon Blue-band Image (Low IM).

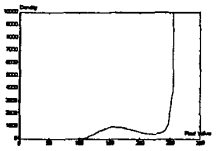

Fig.5(d) : Density Histogram of Fig. 5(a).

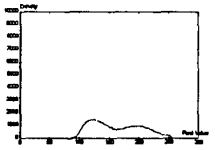

Fig. 5(e) : Density Histogram of Fig. 5(b).

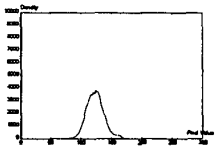

Fig. 5(f) : Density Histogram of Fig. 5(c).

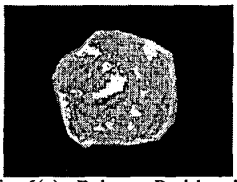

Fig. 6(a) : Polygon Red-band Image (High IM).

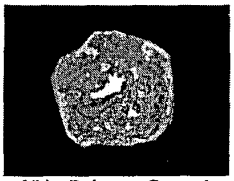

Fig. 6(b) : Polygon Green-band Image (High IM).

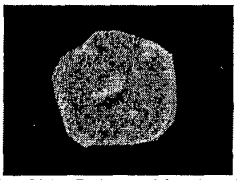

Fig. 6(c) : Polygon blue-band Image (High IM).

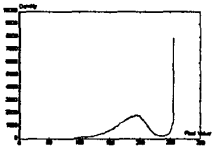

Fig.6(d) : Density Histogram of Fig. 6(a).

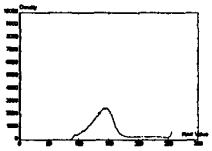

Fig. 6(e) : Density Histogram of Fig. 6(b).

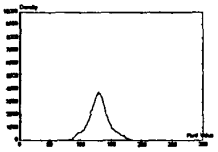

Fig. 6(f) : Density Histogram of Fig. 6(c).

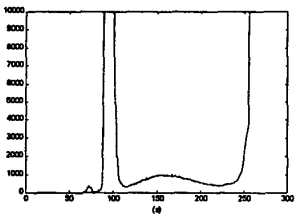

Fig. 7 : Density Histogram of a Circled Red-band Image.

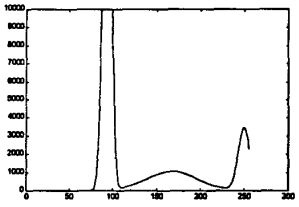

Fig. 8 : 3-components Mixture Normal for Fig. 7.

Table 2 : Proportion Of IM, Mean and Standard Deviation For 3-component Mixture Normal
(Third row represents the estimators of nine parameters after eight iterations)

$\hat{p}_1$	$\hat{p}_2$	$\hat{p}_3$	$\hat{\mu}_1$	$\hat{\mu}_2$	$\hat{\mu}_3$	$\hat{\sigma}_1$	$\hat{\sigma}_2$	$\hat{\sigma}_3$	B-I	G-I	Ratio
0.6	0.3	0.1	90	166	256	2	10	2	114	222	55.21
0.70	0.17	0.13	93	168	250	20	830	43			